



## Plasticized-starch/poly(ethylene oxide) blends prepared by extrusion

Fang Yu<sup>a,b</sup>, Kalappa Prashantha<sup>a,b</sup>, Jeremie Soulestin<sup>a,b,\*</sup>, Marie-France Lacrampe<sup>a,b</sup>, Patricia Krawczak<sup>a,b</sup>

<sup>a</sup> Ecole des Mines de Douai, Polymers and Composites Technology & Mechanical Engineering Department, 941 rue Charles Bourseul, BP 10838, F 59508 Douai, France

<sup>b</sup> Univ. Lille Nord de France, 59000 Lille, France

### ARTICLE INFO

#### Article history:

Received 10 May 2012

Received in revised form 3 August 2012

Accepted 6 August 2012

Available online 10 August 2012

#### Keywords:

Plasticized-starch

Poly(ethylene oxide)

Blends

Extrusion

Morphology

Mechanical properties

### ABSTRACT

Blends based on plasticized-wheat starch (as matrix or rich phase) and poly(ethylene oxide) (PEO) (as dispersed phase) were prepared by melt processing in a twin-screw extruder. The extrusion of the plasticized-starch is significantly facilitated by blending with PEO. Plasticized-starch and PEO are immiscible in the range of the investigated blend ratios (90/10–50/50). The phase inversion takes place when the PEO content is 50 wt.% in the blend. Both the thermal stability and the tensile properties of plasticized-starch are improved by blending with PEO. Also, a synergistic effect between plasticized-starch and PEO is noticed at 25–40 wt.% PEO content in the blend, the Young's modulus of the materials obtained being the highest and higher than both neat polymer components at those blending ratios.

© 2012 Elsevier Ltd. All rights reserved.

### 1. Introduction

Starch is cheap, renewable, naturally biodegradable and widely available in many kinds of plants such as corn, wheat, rice, and potato. Therefore, its use as one of the raw materials for manufacturing sustainable and biodegradable “green” plastic products is of high interest. However, compared to regular oil-based polymers, native starch is not a thermoplastic polymer due to its intra- and inter-molecular hydrogen bonds between hydroxyl groups of starch molecules, which leads to thermally stable crystalline phase. As a consequence, degradation of native starch occurs before melting, which restrains greatly its direct usage in most applications (Chiu & Solarek, 2009). Therefore, it has to be modified or blended with other polymers to be used as a conventional plastic material. Plasticizers are commonly added into native starch in order to transform the semi-crystalline granules into a homogeneous material by destructing hydrogen bonds between the starch granules under shear, leading to the synchronous formation of new hydrogen bonds between plasticizer and starch. Thanks to this process, native starch can be turned into plasticized-starch (TPS). Nevertheless, this thermoplastic material is water sensitive and has poor mechanical properties. So far, studies on

TPS have been intensive to overcome its two main drawbacks. Modifications are often achieved by blending TPS with either non-biodegradable polymers, such as low density polyethylene (LDPE) (Girija & Sailaja, 2006; Ning, Jiugao, Xiaofei, & Ying, 2007; Wang, Yu, & Yu, 2004), or biodegradable polymers, such as poly(lactic acid) (PLA) (Chen et al., 2006; Huneault & Li, 2007; Ke & Sun, 2001; Wang, Yu, Chang, & Ma, 2007, 2008), poly( $\epsilon$ -caprolactone) (PCL) (Avérous, Moro, Dole, & Fringant, 2000; Shin, Lee, Shin, Balakrishnan, & Narayan, 2004), poly(butylene succinate) (PBS) (Zeng et al., 2011), poly(hydroxyalkanoate) (PHA) (Godbole, Gote, Latkar, & Chakrabarti, 2003; Ismail & Gamal, 2010), poly(vinyl alcohol) (PVA) (Rahman, Sin, Rahmat, & Samad, 2010; Sin, Rahmat, Rahman, Sun, & Samad, 2010).

Poly(ethylene oxide) is a biocompatible, low toxic, non-ionic and water soluble polymer with good lubricating, binding and film forming properties (Dhawan, Dhawan, Varma, & Sinha, 2005). It can also retard the release rate of drugs and hence has been widely used in pharmaceutical industries (Dhawan et al., 2005). Therefore, blending of TPS and PEO becomes both scientifically and pharmaceutically interesting due to the biocompatibility of these two hydrophilic polymers.

So far, investigations on blends of PEO and starch have been mostly focused on taking PEO as the matrix and starch as a dispersed phase (Jagadish & Raj, 2011; Pereira, Gouveia, de Carvalho, Rubira, & Muniz, 2009; Pereira et al., 2011; Pereira, Paulino, Rubira, & Muniz, 2010; Pieliowska & Pieliowski, 2010). Pereira et al. (2009, 2010, 2011) investigated the miscibility of PEO/starch blend films obtained by solvent-casting. These authors report the

\* Corresponding author at: Ecole des Mines de Douai, Polymers and Composites Technology & Mechanical Engineering Department, 941 rue Charles Bourseul, BP 10838, F 59508 Douai, France. Tel.: +33 3 2771 2180; fax: +33 3 2771 2981.

E-mail address: [jeremie.soulestin@mines-douai.fr](mailto:jeremie.soulestin@mines-douai.fr) (J. Soulestin).

miscibility of PEO and starch in the case of blends for which starch is the minority phase. Pielichowska et al. reported the phase transition behaviour of the PEO/gelatinized starch blends prepared by solvent-casting with PEO and starch ratios of 3:1, 1:1 and 1:3 (w/w) (Pielichowska & Pielichowski, 2010). The presence of starch changed the PEO phase transition behaviour in relation with a strong intermolecular interaction between starch and PEO (Pielichowska & Pielichowski, 2010). Jagadish and Raj (2011) studied the mechanical, barrier, optical, thermal properties and the surface morphology characteristics of a series of PEO/starch blends (100/0–50/50) prepared using a mixing extruder. This process is an interesting alternative to solvent-casting which is not appropriate for industrial applications.

However to our knowledge, detailed studies on the mechanical, thermal and morphological properties of TPS and PEO blends, particularly in the case of starch-rich blends, have been rarely reported in literature. Besides, both TPS and PEO are biocompatible, biodegradable and hydrophilic, and PEO bears excellent mechanical properties, which are likely to improve the poor mechanical properties of TPS. Furthermore, processing TPS using twin-screw extruder is known to be difficult because of the very high viscosity of starch, and blending with PEO is expected to facilitate the flow behaviour of starch during the extrusion process. Therefore, it seems worth blending TPS and PEO, taking TPS as the matrix, in order to ease the extrusion process and improve the poor mechanical properties of TPS.

The present work aims at preparing such biocompatible and biodegradable blends based on TPS and PEO by melt-extrusion, different contents of PEO being added into the TPS matrix. At first, the miscibility between TPS and PEO was analysed. The effect of introducing PEO into the TPS matrix on the thermal stability and the tensile mechanical properties of TPS was then investigated.

## 2. Experimental

### 2.1. Materials

Wheat starch (Roquette Frères, Lestrem, France) was used in this study. In order to limit fluctuation of humidity in starch, it was stored at 23 °C with 50% relative humidity (RH). In these conditions, the native starch contains 13% of the original moisture. The non-volatile plasticizer was analytical reagent grade glycerol (99% purity, water  $\leq$  1%) (Sigma Aldrich, Saint-Quentin-Fallavier, France). The poly(ethylene oxide) (PEO) homopolymer used had a molecular weight of 300,000 (Polyox WSR-N-750, Dow Europe GmbH, Terneuzen, The Netherlands).

### 2.2. Blends preparation

Starch was dried in a vacuum oven at 80 °C for at least 12 h. The glycerol used as plasticizer was manually premixed with the dry starch at a fixed content of 25 wt.%. After waiting for 1 h to let the plasticizer swell the starch granules in order to enhance the molecular interactions between the plasticizer and starch, the PEO powder was then manually mixed with the pre-mixtures in each desired composition. The obtained mixtures were subsequently fed into a parallel co-rotating laboratory-scale twin-screw extruder (Haake Rheomex PTW 16 OS, Thermo Fisher Scientific, Courtaboeuf, France). The screw diameter was 16 mm with a screw ratio ( $L/D$ ) of 40. The screw speed during the extrusion was 35 rpm. The temperature profile setting along the extruder barrel was 125, 126, 127, 128, 129, 130, 131, 132, 133 and 134 °C (from the hopper to the die) with around 3 °C fluctuation for each temperature zone during the processing. The obtained extrudates were subsequently pelletized after air-cooling on a conveyer belt. For a comparison purpose, neat

**Table 1**

Composition of plasticized starch (TPS)/PEO blends prepared by twin-screw extrusion.

| Sample composition P-St/PEO | TPS           |                 | PEO (wt.%) |
|-----------------------------|---------------|-----------------|------------|
|                             | Starch (wt.%) | Glycerol (wt.%) |            |
| 100/0                       | 75.00         | 25.00           | 0.00       |
| 90/10                       | 67.50         | 22.50           | 10.00      |
| 75/25                       | 56.25         | 18.75           | 25.00      |
| 60/40                       | 45.00         | 15.00           | 40.00      |
| 50/50                       | 37.50         | 12.50           | 50.00      |
| 0/100                       | 0.00          | 0.00            | 100.00     |

plasticized starch (TPS) and PEO samples were also prepared in the same way. The composition of the samples obtained at different blend ratios are reported in Table 1.

The addition of PEO, even at low content, greatly eases the processability of TPS by extrusion, by improving the material feeding and flow properties. This point is particularly interesting as plasticization of starch by extrusion is known to be tricky.

### 2.3. Injection moulding of test samples

After pelletizing and conditioning at 23 °C and 50% RH during 24 h, all materials were injection-moulded (Babypast 6/10P, Cronoplast, Abrera, Italy) into standard test specimen for tensile and dynamic mechanical analysis. The typical injection-moulding conditions were the following: temperature profile setting at 170–175–180 °C (from hopper to nozzle), injection pressure of 150 bars, holding pressure of 130 bars, and cooling time of 25 s. Before testing, all samples were stored in controlled temperature and humidity chamber for one week at 23 °C and 50% RH.

### 2.4. Scanning electron microscopy (SEM)

The fracture surfaces of the materials were observed by scanning electron microscopy (SEM) under high vacuum with a SEM instrument (S-4300SE/N, Hitachi Ltd., Tokyo, Japan) operating at 10 kV, the injection-moulded cryofractured samples being previously coated with a thin gold layer.

### 2.5. Polarized optical microscopy (POM)

The spherulite structure was characterized by polarized optical microscopy (POM) on film sample (obtained by compression moulding at 180 °C during 3 min) using a polarized microscope (DM2500M, Leica Microsystems GmbH, Wetzlar, Germany) equipped with a hot stage device (FP80, Mettler-Toledo, Würit, Germany) and a camera (DFC420, Leica). The film sample was sandwiched between two glass slides. After melting at 180 °C for 2 min, it was quickly quenched to the room temperature (23 °C). The formation of the spherulite morphology was then monitored.

### 2.6. Fourier transform infrared (FT-IR) spectroscopy

Infrared spectra of the samples were recorded on 50  $\mu$ m thick sample slices cut with a microtome (Leica RM2165, Leica Microsystems, Heerbrugg, Switzerland) using a Fourier transform infrared (FT-IR) spectrometer (Nicolet 380, Thermo Fisher Scientific, Courtaboeuf, France) under atmospheric conditions. The spectra were recorded using at least 128 scans with 2  $\text{cm}^{-1}$  resolution, in the spectral range 400–4000  $\text{cm}^{-1}$ . The measurement was conducted in attenuated total reflectance (ATR) mode.

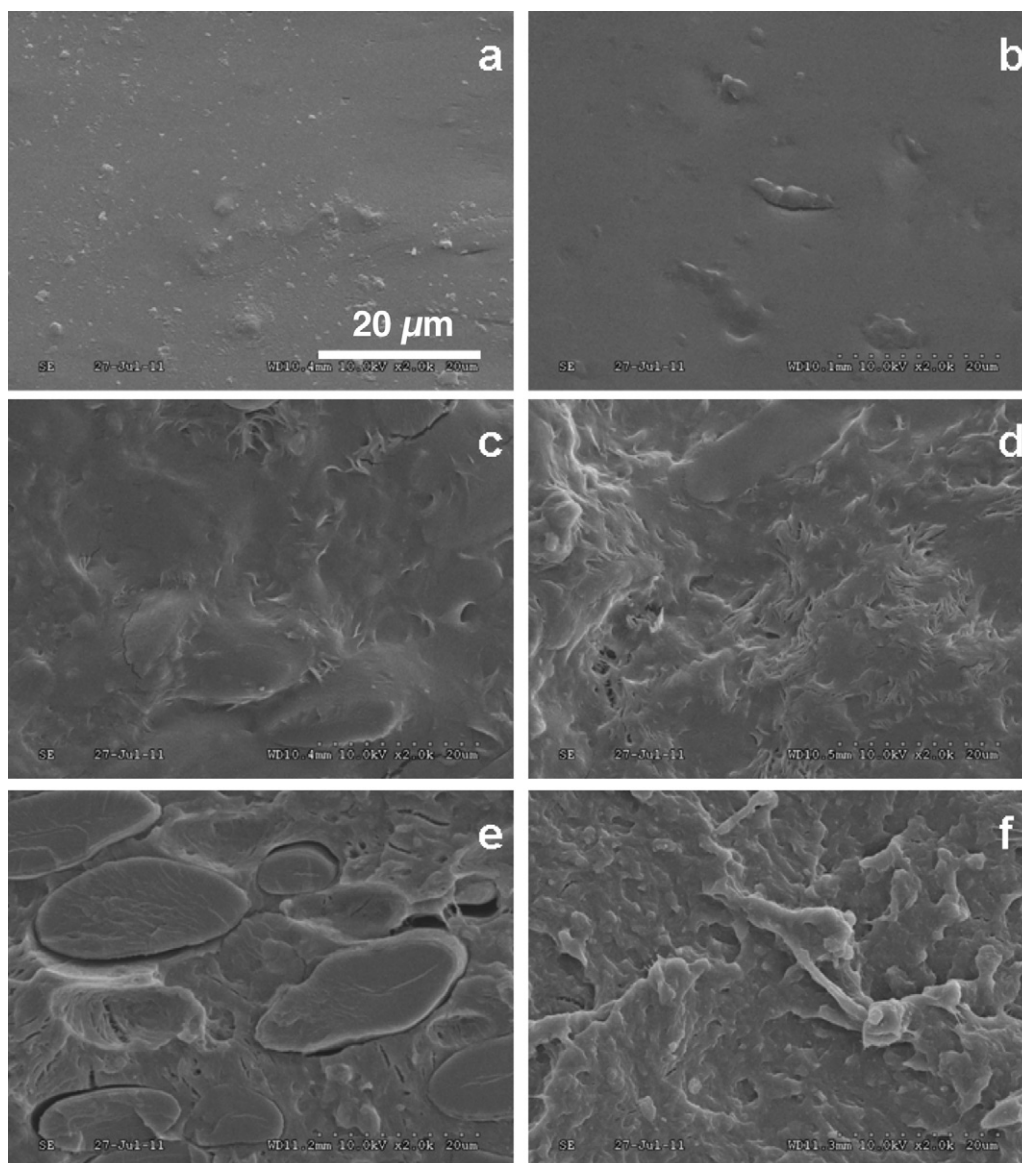


**Fig. 1.** SEM images of cryofractured surfaces of (a) neat plasticized starch (TPS), TPS/PEO blends with PEO content of (b) 10 wt.%, (c) 25 wt.%, (d) 40 wt.%, (e) 50 wt.%, and (f) neat PEO. Scale bar for (a)–(f): 20  $\mu\text{m}$ .

### 2.7. Differential scanning calorimetry (DSC)

The differential scanning calorimetry (DSC) thermograms were recorded using a device equipped with liquid nitrogen cooling (DSC 8500, Perkin Elmer, Courtaboeuf, France). The sample (around 10 mg) was pre-sealed into an aluminium pan. The sample was first held at  $-90^{\circ}\text{C}$  for 5 min for stabilization, and was then heated to  $150^{\circ}\text{C}$  at a constant heating rate of  $40^{\circ}\text{C min}^{-1}$  (first heating scan). After holding for 3 min at  $180^{\circ}\text{C}$ , the sample was subsequently cooled to  $-90^{\circ}\text{C}$  at a cooling rate of  $-10^{\circ}\text{C min}^{-1}$  (cooling scan). After holding at  $-90^{\circ}\text{C}$  for 3 min, the sample was heated again to  $150^{\circ}\text{C}$  at a constant heating rate of  $40^{\circ}\text{C min}^{-1}$  (second heating scan).

### 2.8. Dynamic mechanical analysis (DMA)

The viscoelastic behaviour was studied in tension by dynamic mechanical analysis (DMA+ 150, MetraviB, Limonest, France) at a frequency of 10 Hz. Data were collected from  $-100$  to  $150^{\circ}\text{C}$  at a heating rate of  $2^{\circ}\text{C min}^{-1}$ . DMA specimens

(4 mm  $\times$  10 mm  $\times$  15 mm) were cut from injection-moulded samples.

### 2.9. Thermo-gravimetric analysis (TGA)

The thermal stability of the samples was measured with a thermogravimetric analyzer (TGA 7, Perkin Elmer, Courtaboeuf, France). The sample (around 10 mg) was heated from 30 to  $600^{\circ}\text{C}$  at a heating rate of  $10^{\circ}\text{C min}^{-1}$  in a nitrogen atmosphere with a purge flow rate of  $20\text{ ml min}^{-1}$ .

### 2.10. Tensile behaviour

The mechanical properties were evaluated from injection-moulded dumbbell-shaped specimens (gauge length of 50 mm and thickness of  $2.80 \pm 0.15\text{ mm}$ ). Tensile properties were measured using a tensile machine (Lloyd LR50K, Ametek, Elancourt, France) equipped with a 1 kN force sensor at a crosshead speed of  $10\text{ mm min}^{-1}$  at  $23^{\circ}\text{C}$  and 50% RH according to the ISO 527 standard. At least five specimens of each composition were tested.



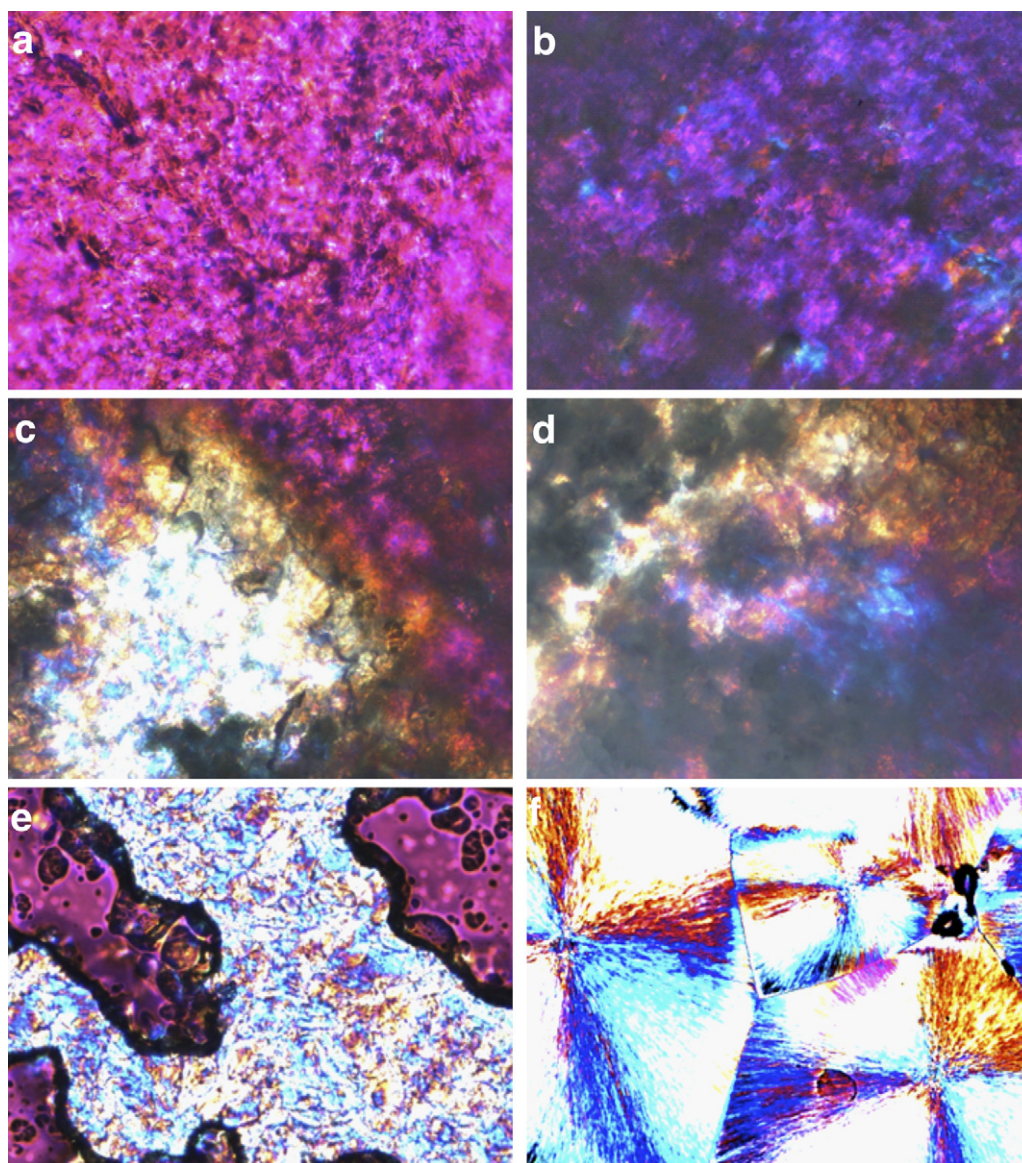


**Fig. 2.** Spherulite morphology of (a) neat plasticized starch (TPS), TPS/PEO blends with PEO content of (b) 10 wt.%, (c) 25 wt.%, (d) 40 wt.%, (e) 50 wt.%, and (f) neat PEO after full crystallization at 23 °C. Scale bar for (a)–(f): 50  $\mu$ m.

### 3. Results and discussion

#### 3.1. Fracture surface morphology

The cryofractured surface morphology of neat TPS and TPS/PEO blends observed by SEM are shown in Fig. 1. A continuous phase with only few residual granules is observed for neat TPS plasticized with 25 wt.% of glycerol (Fig. 1a), indicating that the incorporation of 25 wt.% glycerol plasticizer can effectively disrupt the inter-molecular and intramolecular hydrogen bonds of native wheat starch under the high shear and temperature conditions of the twin-screw extruder. Recently, using X-Ray Diffraction, our group has demonstrated the efficiency of twin-screw extrusion using similar conditions to destructure granules and plasticize native starch (Schmitt, Prashantha, Soulestin, Lacrampe, & Krawczak, 2012). The blend containing 10 wt.% PEO shows (Fig. 1b) a surface morphology similar to that of neat TPS, with extra small bumps. When PEO content reaches 25 and 40 wt.%, a fibrillar structure was observed (Fig. 1c and d). At 50 wt.% PEO (Fig. 1e), the surface morphology becomes significantly different and obvious nodular

morphology is observed. Considering the surface morphology of neat PEO (Fig. 1f), it seems that the phase inversion takes place when PEO content reaches 50 wt.%, and a co-continuous morphology is obtained for this blend. According to the small bump structure, the fibrillar and nodular structure observed with increasing PEO content in the blend, it is likely that TPS is at least partially immiscible with PEO in the range of the investigated blend ratios.

#### 3.2. Spherulite morphology

The phase morphology of the samples was further investigated using POM (Fig. 2). Almost no crystalline structure of starch granules can be observed for neat TPS (Fig. 2a), indicating that the processing of starch can effectively destroy the granular structure of the native starch leading to an amorphous plasticized-starch. Neat PEO exhibits spherulites with typical Maltese cross pattern (Fig. 2f), which are in close contact indicating the high crystallinity of PEO. The blend containing 10 wt.% PEO shows morphology similar to that of neat TPS, however some domains of higher brightness can be observed (Fig. 2b). Similar trends are also observed for the blends

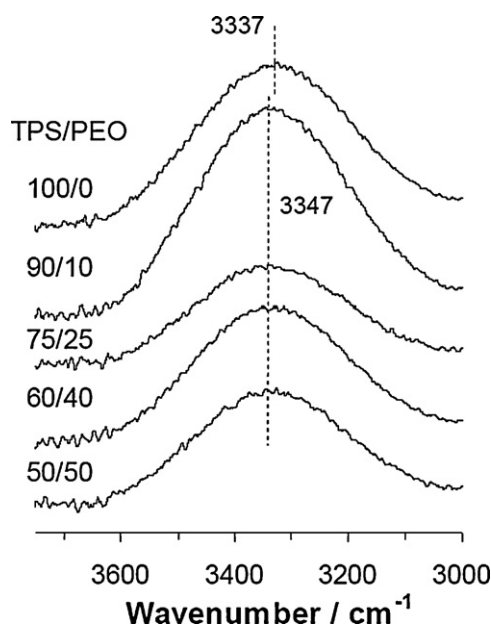


Fig. 3. FTIR spectra of hydroxyl absorption of (a) neat plasticized starch (TPS), TPS/PEO blends.

containing 25 and 40 wt.% PEO (Fig. 2c and d, respectively) with increase in brightness (coloured domains) and spherulites size. It is suggested that this enhanced brightness is more inclined to be caused by the birefringence of the PEO crystalline phase indicating that PEO component crystallizes in the TPS matrix. At 50 wt.% PEO (Fig. 2e), the phase morphology is completely different. A typical co-continuous morphology is observed. The above results further support that TPS is not miscible with PEO in the range of the investigated blend ratios.

### 3.3. Molecular interactions analysis

FT-IR spectroscopy provides information about molecular interactions, and consequently it is useful to detect the existence of the hydrogen-bonding or other specific interactions in polymer blend systems. If PEO is miscible with TPS, the hydrogen bonding of TPS must be disturbed and the conformational structures have to be changed in the blend (Kim, Kim, & Cho, 2009).

The FT-IR spectra corresponding to the stretching vibrations of the hydroxyl group in the region of 3700–3000  $\text{cm}^{-1}$  were recorded (Fig. 3). Compared to neat TPS, the blend containing 10 wt.% PEO exhibits a slight spectral shift from 3337 to 3347  $\text{cm}^{-1}$ , whereas with increasing PEO content from 10 to 50 wt.%, no noticeable spectral shift can be observed. This indicates that there are almost no molecular interactions between TPS and PEO or if there is, the molecular interactions between them should be very weak. It is probably because the interactions between the starch molecules and the glycerol plasticizer are much stronger, leading to very weak molecular interactions between starch and PEO. The lack of compatibility between PEO and plasticized starch tends to prove that the improved processability observed during extrusion of the blends is not due to a co-plasticizing effect of PEO. However, the presence of PEO, a thermoplastic polymer can ease starch plasticization with glycerol during extrusion process.

### 3.4. Thermal behaviour

To further investigate the miscibility between TPS and PEO, a DSC analysis was conducted. Experimentally, miscibility of polymer

**Table 2**

Glass transition ( $T_g$ ), crystallization ( $T_c$ ) and melting ( $T_m$ ) temperatures, and melting enthalpy  $\Delta H_m$  of plasticized starch (TPS)/PEO blends.

| Sample composition TPS/PEO | $T_g$ ( $^{\circ}\text{C}$ ) | PEO                          |                              |                                      |
|----------------------------|------------------------------|------------------------------|------------------------------|--------------------------------------|
|                            |                              | $T_c$ ( $^{\circ}\text{C}$ ) | $T_m$ ( $^{\circ}\text{C}$ ) | $\Delta H_m^a$ ( $\text{J g}^{-1}$ ) |
| 100/0                      | −54.3                        | –                            | –                            | –                                    |
| 90/10                      | −52.5                        | 34.6                         | 64.6                         | 99.5                                 |
| 75/25                      | −49.4                        | 35.7                         | 71.1                         | 138.1                                |
| 60/40                      | −49.3                        | 37.5                         | 72.6                         | 138.7                                |
| 50/50                      | −50.4                        | 38.4                         | 72.9                         | 142.3                                |
| 0/100                      | −52.8                        | 40.5                         | 79.6                         | 148.0                                |

<sup>a</sup> Heat of fusion normalized by blend composition.

blends is usually assessed on the basis of the existence of a single  $T_g$  measured by DSC or DMA.

Over the years, many equations have been suggested for predicting the variation of the  $T_g$  of a miscible blend as a function of blend composition, such as Fox (1956), Gordon–Taylor (Gordon & Taylor, 1952) or Kwei (1984) equations. Fox equation is the most basic and popular one to characterize the additive behaviour of the  $T_g$  of the polymeric system in a rough approximation. Gordon–Taylor equation is suitable for a miscible system with weak intermolecular interactions while Kwei equation is usually used for a system with very strong intermolecular interactions. As FT-IR analysis reveals that there are almost no molecular interactions between TPS and PEO. Further, the Gordon–Taylor equation was used to show the lack of miscibility between the TPS and the PEO. It is expressed as

$$T_g^{\text{blend}} = \frac{[W_a T_g^a + K W_b T_g^b]}{[W_a + K W_b]}$$

where  $W_a$  and  $W_b$  are the weight fraction of polymer a and b, respectively.  $T_g^a$  and  $T_g^b$  are the glass transition temperature of polymer a and b, respectively (Gordon & Taylor, 1952). The parameter  $K$  is the ratio of the volume expansion coefficients of the components at the glass transition temperature (Gordon & Taylor, 1952) or the ratio of the heat capacity increments (Lin, Kwei, & Reiser, 1989) of the components during the glass transition.

Fig. 4a–c shows the DSC diagrams of the first heating, then cooling and second heating scans. Fig. 4d is the differentiated DSC (DDSC) curve of the second heating scan. The glass transition temperature ( $T_g$ ) of the blends, the crystallization temperature ( $T_c$ ), the melting point ( $T_m$ ) as well as the heat of fusion ( $\Delta H_m$ ) of the PEO component are summarized in Table 2. The  $T_g$  was taken as an inflection point in the jump of the heat capacity in the second heating scan (maximum of the peak of DDSC curve). No significant melting transitions were detected for TPS. Moreover, due to the presence of the small molecules such as glycerol plasticizer and water, some instabilities appeared during the first heating scan of TPS with increasing temperature, which is due to increase in pressure caused by the evaporation of these small molecules. On the opposite, when TPS is blended with PEO, obvious melting and crystallization peaks can be detected in the heating and cooling curves.

The  $T_g$  values were then plotted against the blend composition (Fig. 5). The solid line represents the theoretically calculated  $T_g$  from the Gordon–Taylor equation. The parameter  $K$  was calculated as the ratio of the heat capacity increments of TPS and PEO during the glass transition. The  $T_g$  values of the blends deviate significantly from those calculated from the Gordon–Taylor equation for miscible blends. A single peak is observed corresponding to the  $T_g$  resulting from the convolution of both relaxations of PEO and TPS. This convolution tends to increase the value of resulting single peak. This result further confirms that the TPS and PEO are not miscible in the range of the investigated blend ratios.

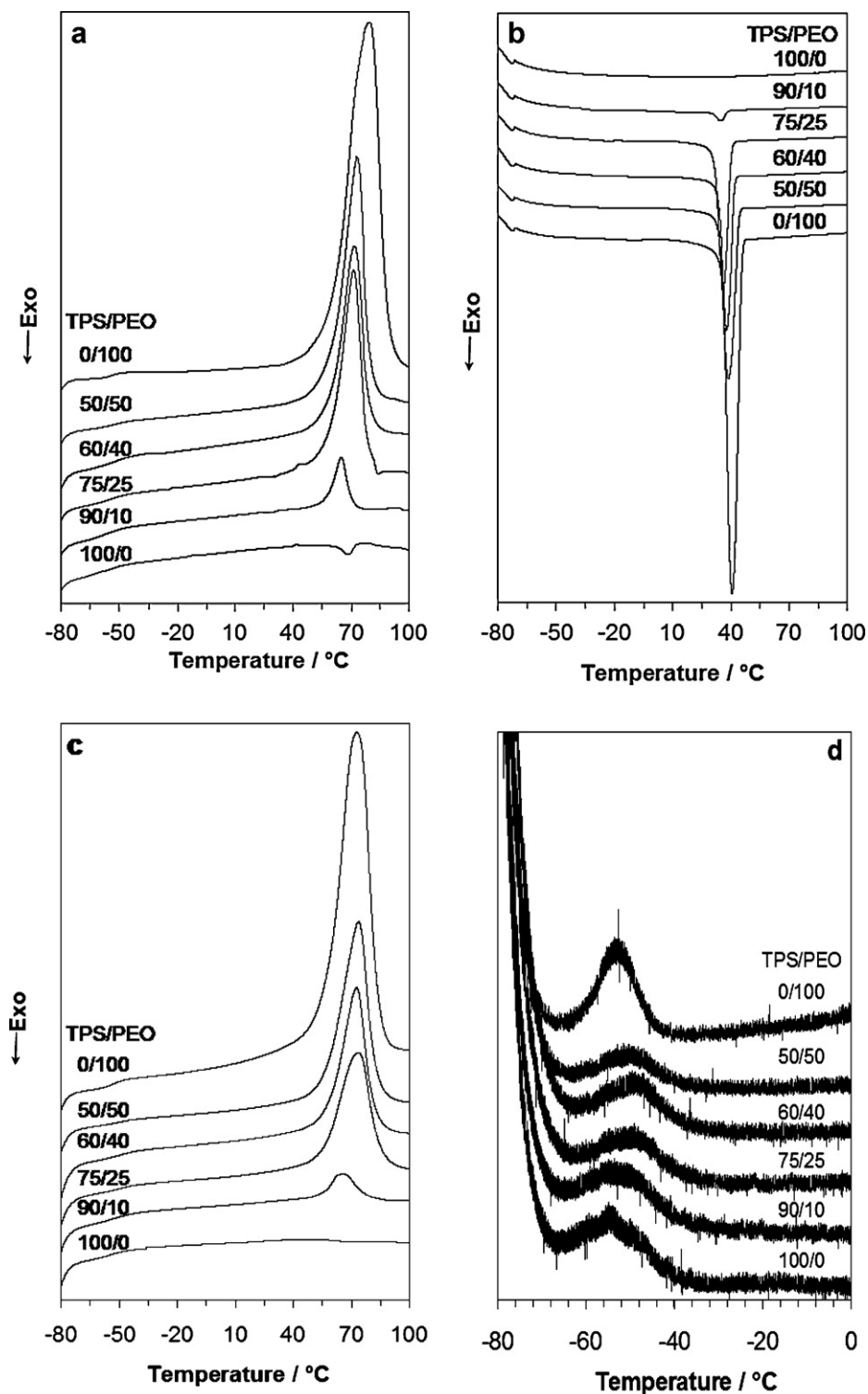


**Fig. 4.** DSC thermograms of plasticized starch (TPS)/PEO blends: (a) first heating scan ( $40^{\circ}\text{C min}^{-1}$ ), (b) cooling scan ( $-10^{\circ}\text{C min}^{-1}$ ), (c) second heating scan ( $40^{\circ}\text{C min}^{-1}$ ), and (d) differentiated DSC curve of second heating scan.

Moreover, the appearance of the crystallization peaks at all blend ratios corroborates well the POM analysis. The increase of the crystallization temperature, the melting point as well as the heat of fusion of the PEO component with increasing PEO content in the blend indicates that PEO can form more and more perfect crystals and its crystallinity gradually increases. These results are also signs of phase separation which supports the immiscibility between TPS and PEO in the range of the investigated blend ratios.

### 3.5. Thermal stability

Processability and applicability of polymer systems depends greatly on their thermal stability. Thermogravimetric analysis (TGA) was consequently conducted. The TGA traces and the corresponding derivative curves are shown in Fig. 6. PEO exhibits an obvious one-step weight loss mechanism and is much more thermally stable than TPS. For TPS, a two-step weight loss mechanism



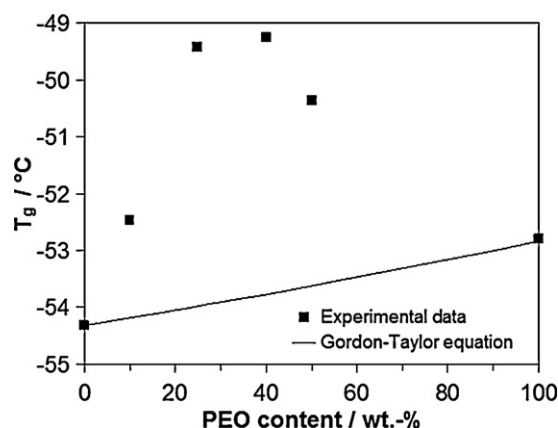


**Fig. 5.** Glass transition temperature ( $T_g$ ) of plasticized starch (TPS)/PEO blends. The solid line indicates the theoretical values calculated by the Gordon–Taylor equation.

is observed. The first step corresponds to the loss of the volatiles components including the water and glycerol. The initial weight loss of water starts just above the room temperature, and the weight loss of glycerol starts at around 180 °C (Vega, Villar, Failla, & Vallés, 1996). The second step in the approximate range of 250–350 °C is related to the pyrolysis of starch (Kwei, 1984). In the case of the blends, three-step weight loss mechanism is observed, that is, the loss of the volatiles, pyrolysis of starch and pyrolysis of PEO, respectively.

Table 3 summarizes the peak position of the maximum weight loss ( $T_{max}$ ) and the degradation extent (DE) for the neat TPS, PEO and their blends. As the degradation of starch and PEO is

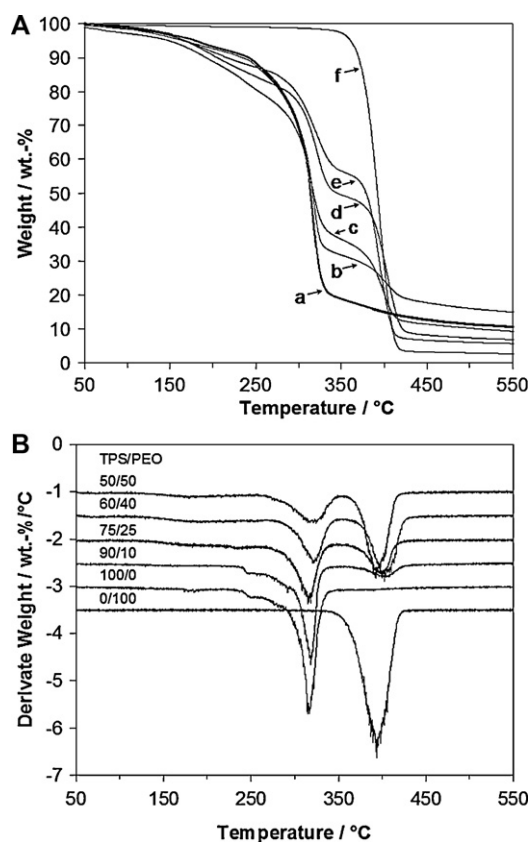


**Fig. 6.** Thermogravimetric weight loss curves (A) and derivated curves (B) monitored at 10 °C min<sup>−1</sup> under the nitrogen atmosphere for: (a) neat plasticized starch (TPS), TPS/PEO blends with PEO content of (b) 10 wt.%, (c) 25 wt.%, (d) 40 wt.%, (e) 50 wt.%, and (f) neat PEO.

**Table 3**

Temperature of maximum rate of weight loss ( $T_{max}$ ) and degradation extent (DE) of plasticized starch (TPS)/PEO blends.

| Sample composition TPS/PEO | <350 °C        |        | >350 °C        |        |
|----------------------------|----------------|--------|----------------|--------|
|                            | $T_{max}$ (°C) | DE (%) | $T_{max}$ (°C) | DE (%) |
| 100/0                      | 317            | 56     | –              | –      |
| 90/10                      | 319            | 54     | 404            | 77     |
| 75/25                      | 317            | 49     | 401            | 80     |
| 60/40                      | 323            | 39     | 404            | 75     |
| 50/50                      | 322            | 33     | 393            | 68     |
| 0/100                      | –              | –      | 394            | 55     |

observed separately in the case of the blends, it shows the lack of compatibility between the two phases as already reported by Sreekumar, Al-Harathi, and De (2011, 2012). The  $T_{max}$  corresponding to the pyrolysis of starch shifts to relatively higher temperature with increasing PEO content in the blend, although the shift is not linearly dependent on the blend ratio. It is considered that the presence of PEO in the blend may probably act as a depolymerisation-retardant as PEO is more thermally stable, can retard the depolymerisation of starch molecules (Yu, Nakamura, & Inoue, 2010). It also indicates that the thermal stability of TPS can be improved by blending with PEO, the improvement effect being not linearly dependent on the blend ratio, which is assumed to be caused by the different morphology of the blend samples with different PEO content.

### 3.6. Viscoelastic properties

Fig. 7a and b shows respectively the loss factor  $\tan \delta$  and the storage modulus  $E'$  of the neat materials and the blends as a function of the temperature. As the melting point of PEO is in the range of 70–80 °C according to DSC analysis, both the  $\tan \delta$  and the storage modulus  $E'$  curves were recorded in the temperature range of −65 to 55 °C.

The  $T_g$  of neat TPS is around −34.6 °C, which is ascribed to the starch-poor phase (Forssell, Mikkilä, Moates, & Parker, 1997). The  $T_g$  of neat PEO is around −44.6 °C. When blending TPS with 10, 25, 40 and 50 wt.% PEO, no obvious shift in peak position (respectively −34.6, −36.4, −35.2, and −36.5 °C) can be observed for the  $T_g$  attributed to the starch-poor phase of TPS. The shape of the transition peak tends to broaden with increasing PEO content in the blend, which is suggested to be due to the convolution of TPS and PEO relaxation peaks. These results confirm the previous conclusions drawn from DSC analysis.

The values of storage modulus ( $E'$ ) also provide some relevant indications on the stiffness properties. The storage modulus of the blends below  $T_g$  is much higher than that of neat TPS and PEO (Fig. 7b). For all samples, the  $E'$  values decrease greatly after the  $T_g$ . In order to evaluate the effect of the PEO content on the modulus of the blends, the  $E'$  values at −60, 10 and 50 °C, where PEO is in glassy, amorphous and close to melt state, respectively, were plotted against the PEO content (Fig. 7c). The  $E'$  values of the blends are significantly higher than those of the neat materials at corresponding temperature, revealing that there is a synergistic effect between PEO and TPS. Actually, even if the two phases have storage moduli close to each other a significant reinforcement effect is observed when blending PEO and TPS.

### 3.7. Mechanical properties in tension

In order to confirm these trends, tensile tests were also performed. Fig. 8 shows the stress–strain curves of the neat TPS, PEO and their blends. The corresponding tensile properties are summarized in Table 4. TPS is less ductile than PEO. When blending

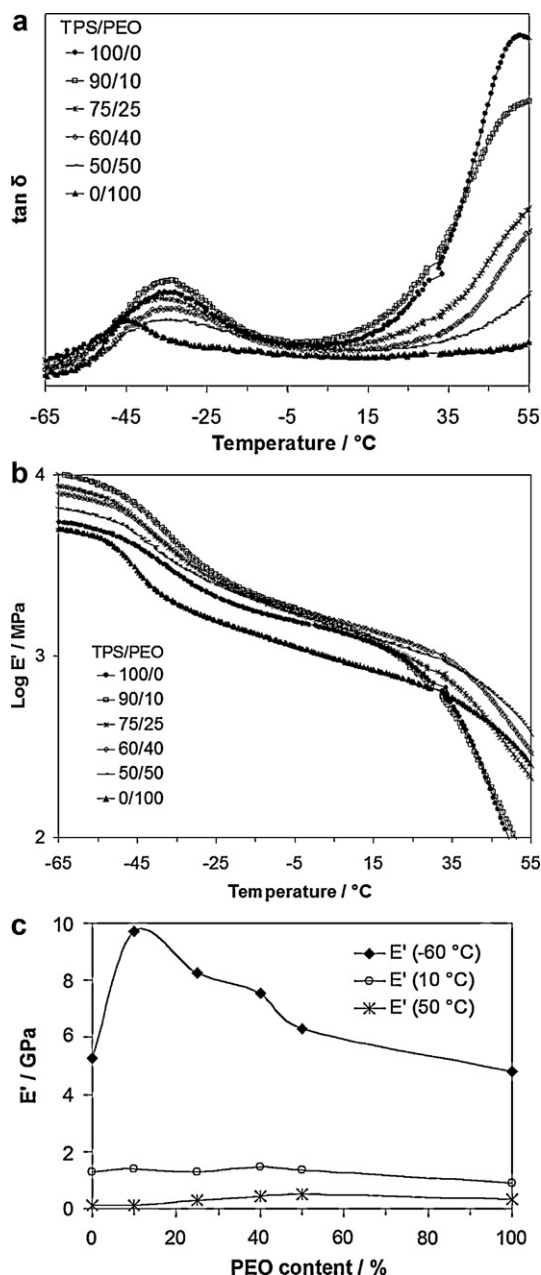


**Fig. 7.** Viscoelastic properties of plasticized starch (TPS)/PEO blends: (a)  $\tan \delta$  and (b) storage modulus  $E'$  versus temperature, and (c) storage modulus  $E'$  at  $-60$ ,  $10$  and  $50$  °C versus PEO content.

TPS with 10 wt.% PEO, the Young's modulus hardly decreases (considering data scattering) and the strain at break significantly decreases. This may be ascribed to the absence of molecular interactions between TPS and PEO, leading to a phase separation and

**Table 4**  
Young's modulus, tensile yield stress and strain at break of plasticized starch (TPS)/PEO blends.

| Sample composition<br>TPS/PEO | Young's modulus<br>(MPa) | Yield stress<br>(MPa) | Strain at break<br>(%) |
|-------------------------------|--------------------------|-----------------------|------------------------|
| 100/0                         | $587.2 \pm 41.4$         | $12.3 \pm 0.4$        | $45.1 \pm 2.8$         |
| 90/10                         | $557.5 \pm 23.0$         | $11.3 \pm 0.2$        | $14.8 \pm 1.5$         |
| 75/25                         | $718.8 \pm 26.3$         | $11.2 \pm 0.6$        | $3.5 \pm 0.1$          |
| 60/40                         | $700.3 \pm 16.4$         | $11.6 \pm 0.3$        | $4.1 \pm 0.3$          |
| 50/50                         | $597.5 \pm 30.1$         | $8.6 \pm 0.6$         | $134.0 \pm 17.3$       |
| 0/100                         | $564.6 \pm 10.8$         | $12.8 \pm 0.1$        | $186.5 \pm 15.5$       |

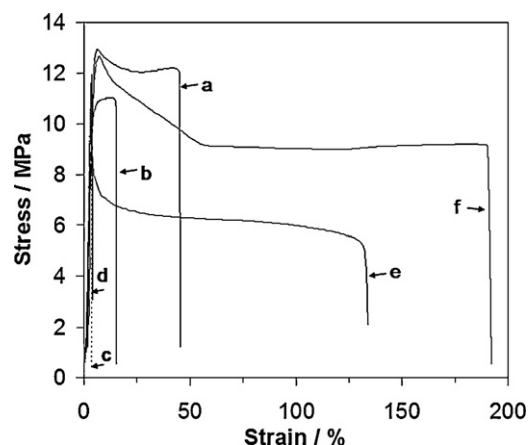


**Fig. 8.** Stress-strain curves of (a) neat plasticized starch (TPS), TPS/PEO blends.

resulting in debonding at the interface. By further increasing the PEO content to 25 wt.%, the strain at break further drops, while the Young's modulus increases significantly. Similar trend is also noticed for the blend with 40 wt.% PEO. The significantly increased Young's modulus of these two samples further confirms the synergy effect obtained by blending PEO and TPS in terms of stiffness improvement, which has been already established by DMA analysis. The transition from ductile to brittle behaviour upon addition of PEO for the blends containing 25 and 40 wt.% PEO is attributed to the heterogeneous morphology due to the immiscibility of TPS and PEO. The lack of compatibility leads to phase debonding that induces early damage of the blends. The blend containing 50 wt.% PEO exhibits a Young's modulus similar to that of neat PEO (considering data scattering) and an increase in strain at break, which becomes comparable to that of neat PEO. This improvement is explained by the phase inversion that occurs for this blend ratio, probably due to the co-continuous morphology formed at this blend ratio. PEO tends to replace TPS as a matrix leading to higher ductility. Similar trends were reported elsewhere in the literature (Lyngaae Jørgenson & Søndergaard, 1987; Sperling, 1976). The blend containing 50 wt.% PEO is a good compromise from application point of view, as it offers both slightly improved stiffness and higher ductility compared to TPS.

#### 4. Conclusions

Elaboration of biocompatible and biodegradable blends of glycerol-plasticized-starch, as rich phase, and poly(ethylene oxide) (PEO) by melt extrusion in a twin-screw extruder was reported for the first time. As expected, the extrusion condition of the plasticized-starch in the twin-screw extruder is significantly facilitated by blending with PEO even at low content. Plasticized-starch and PEO are not miscible in the range of investigated blend ratios. The PEO phase appears as a dispersed phase in plasticized-starch matrix and phase inversion takes place when PEO content is 50 wt.%. There are almost no molecular interactions between plasticized-starch and PEO, probably due to the strong molecular interactions between the starch and its glycerol plasticizer.

Both the thermal stability and the stiffness of plasticized-starch are improved by blending with PEO, the improvement effect being not linearly dependent on the blend ratios. The stiffness of plasticized-starch reaches a maximum value upon addition of 25–40 wt.% PEO, showing a synergy effect between plasticized-starch and PEO, at the expense of ductility. Due to phase inversion, the plasticized-starch/PEO blend with the blend ratio of 50/50 is much more ductile. These results are of prime interest, showing that the addition of PEO in plasticized-starch greatly improves



both the processability and the usage properties of thermoplastic starch materials. As a consequence such compounds may expect promising applications in both medical field, because of their biocompatibility, and food packing field as eco-friendly biodegradable materials.

## Acknowledgements

The authors are indebted to the French Ministry of Economy, Finance and Industry (MATORIA project, Contract no. 08 2 90 6249) to CISIT (International Campus on Safety and Intermodality in Transportation), the Nord-Pas-de-Calais Region and the European Community (FEDER, European Funds for Regional Development) for their financial support.

## References

- Avérus, L., Moro, L., Dole, P., & Fringant, C. (2000). Properties of thermoplastic blends: Starch-polycaprolactone. *Polymer*, 41(11), 4157–4167.
- Chen, L., Qiu, X., Xie, Z., Hong, Z., Sun, J., Chen, X., et al. (2006). Poly(L-lactide)/starch blends compatibilized with poly(L-lactide)-g-starch copolymer. *Carbohydrate Polymers*, 65(1), 75–80. <http://dx.doi.org/10.1016/j.carbpol.2005.12.029>
- Chiu, C., & Solarek, D. (2009). In R. Whistler, & J. BeMiller (Eds.), *Starch Chemistry and Technology*. New York: Academic Press.
- Dhawan, S., Dhawan, K., Varma, M., & Sinha, V. R. (2005). Applications of poly(ethylene oxide) in drug delivery systems. Part II. *Pharmaceutical technology*, 29(9), 82–96.
- Forssell, P., Mikkilä, J., Moates, G., & Parker, R. (1997). Phase and glass transition behaviour of concentrated barley starch–glycerol–water mixtures, a model for thermoplastic starch. *Carbohydrate Polymers*, 34(4), 275–282.
- Fox, T. (1956). The influence of diluent and of copolymer composition on the glass temperature of a polymer system. *Bulletin of the American Physical Society*, 1, 123–135.
- Girija, B., & Sailaja, R. (2006). Low-density polyethylene/plasticized tapioca starch blends with the low-density polyethylene functionalized with maleate ester: Mechanical and thermal properties. *Journal of Applied Polymer Science*, 101(2), 1109–1120.
- Godbole, S., Gote, S., Latkar, M., & Chakrabarti, T. (2003). Preparation and characterization of biodegradable poly-3-hydroxybutyrate–starch blend films. *Bioresource Technology*, 86(1), 33–37.
- Gordon, M., & Taylor, J. S. (1952). Ideal copolymers and the second-order transitions of synthetic rubbers. I. Non-crystalline copolymers. *Journal of Applied Chemistry*, 2, 493–500.
- Huneault, M. A., & Li, H. (2007). Morphology and properties of compatibilized polylactide/thermoplastic starch blends. *Polymer*, 48(1), 270–280. <http://dx.doi.org/10.1016/j.polymer.2006.11.023>
- Ismail, A. M., & Gamal, M. A. B. (2010). Water resistance, mechanical properties, and biodegradability of poly(3-hydroxybutyrate)/starch composites. *Journal of Applied Polymer Science*, 115(5), 2813–2819. <http://dx.doi.org/10.1002/app.31181>
- Jagadish, R. S., & Raj, B. (2011). Properties and sorption studies of polyethylene oxide–starch blended films. *Food Hydrocolloids*, 25(6), 1572–1580. <http://dx.doi.org/10.1016/j.foodhyd.2011.01.009>
- Ke, T., & Sun, X. (2001). Effects of moisture content and heat treatment on the physical properties of starch and poly (lactic acid) blends. *Journal of Applied Polymer Science*, 81(12), 3069–3082.
- Kim, C.-H., Kim, D.-W., & Cho, K. Y. (2009). The influence of PEG molecular weight on the structural changes of corn starch in a starch/PEG blend. *Polymer Bulletin*, 63(1), 91–99. <http://dx.doi.org/10.1007/s00289-009-0065-8>
- Kwei, T. K. (1984). The effect of hydrogen bonding on the glass transition temperatures of polymer mixtures – 2003 – Wiley Online Library. *Journal of Polymer Science: Polymer Letters Edition*, 22(6), 307–313. Available from <http://onlinelibrary.wiley.com/doi/10.1002/pol.1984.130220603/Abstract>. Accessed 27.04.12.
- Lin, A. A., Kwei, T. K., & Reiser, A. (1989). On the physical meaning of the Kwei equation for the glass transition temperature of polymer blends. *Macromolecules*, 22(10), 4112–4119. <http://dx.doi.org/10.1021/ma00200a052>
- Lyngaae Jørgensen, J., & Søndergaard, K. (1987). Phase transitions during shear flow of two-phase polymer blends. I. Theory. Transition to homogeneous melt state. *Polymer Engineering and Science*, 27(5), 344–350.
- Ning, W., Jiugao, Y., Xiaofei, M., & Ying, W. (2007). The influence of citric acid on the properties of thermoplastic starch/linear low-density polyethylene blends. *Carbohydrate Polymers*, 67(3), 446–453.
- Pereira, A. G. B., Gouveia, R. F., de Carvalho, G. M., Rubira, A. F., & Muniz, E. C. (2009). Polymer blends based on PEO and starch: Miscibility and spherulite growth rate evaluated through DSC and optical microscopy. *Materials Science and Engineering C*, 29(2), 499–504.
- Pereira, A. G. B., Paulino, A. T., Nakamura, C. V., Britta, E. A., Rubira, A. F., & Muniz, E. C. (2011). Effect of starch type on miscibility in poly(ethylene oxide)/starch blends and cytotoxicity assays. *Materials Science & Engineering C—Materials for Biological Applications*, 31(2), 443–451. <http://dx.doi.org/10.1016/j.msec.2010.11.004>
- Pereira, A., Paulino, A., Rubira, A., & Muniz, E. (2010). Polymer–polymer miscibility in PEO/cationic starch and PEO/hydrophobic starch blends. *Express Polymer Letters*, 4, 488–499.
- Pielichowska, K., & Pielichowski, K. (2010). Novel biodegradable form stable phase change materials: Blends of poly(ethylene oxide) and gelatinized potato starch. *Journal of Applied Polymer Science*, 116(3), 1725–1731. <http://dx.doi.org/10.1002/app.31615>
- Rahman, W. A. W. A., Sin, L. T., Rahmat, A. R., & Samad, A. A. (2010). Thermal behaviour and interactions of cassava starch filled with glycerol plasticized polyvinyl alcohol blends. *Carbohydrate Polymers*, 81(4), 805–810. <http://dx.doi.org/10.1016/j.carbpol.2010.03.052>
- Schmitt, H., Prashantha, K., Soulestin, J., Lacrampe, M. F., & Krawczak, P. (2012). Preparation and properties of novel melt-blended halloysite nanotubes/wheat starch nanocomposites. *Carbohydrate Polymers*, 89(3), 920–927. <http://dx.doi.org/10.1016/j.carbpol.2012.04.037>
- Shin, B. Y., Lee, S. I. I., Shin, Y. S., Balakrishnan, S., & Narayan, R. (2004). Rheological, mechanical and biodegradation studies on blends of thermoplastic starch and polycaprolactone. *Polymer Engineering and Science*, 44(8), 1429–1438.
- Sin, L. T., Rahmat, A. R., Rahman, W. A. W. A., Sun, Z.-Y., & Samad, A. A. (2010). Rheology and thermal transition state of polyvinyl alcohol–cassava starch blends. *Carbohydrate Polymers*, 81(3), 737–739. <http://dx.doi.org/10.1016/j.carbpol.2010.03.044>
- Sperling, L. (1976). Phase structure and continuity in polymer blends and composites. *Polymer Engineering and Science*, 16(2), 87–92.
- Sreekumar, P. A., Al-Harthi, M. A., & De, S. K. (2011). Effect of glycerol on thermal and mechanical properties of polyvinyl alcohol/starch blends. *Journal of Applied Polymer Science*, 123(1), 135–142. <http://dx.doi.org/10.1002/app.34465>
- Sreekumar, P. A., Al-Harthi, M. A., & De, S. K. (2012). Studies on compatibility of biodegradable starch/polyvinyl alcohol blends. *Polymer Engineering and Science*, <http://dx.doi.org/10.1002/pen.23178>
- Vega, D., Villar, M. A., Failla, M. D., & Vallés, E. M. (1996). Thermogravimetric analysis of starch-based biodegradable blends. *Polymer Bulletin*, 37(2), 229–235. <http://dx.doi.org/10.1007/BF00294126>
- Wang, N., Yu, J., Chang, P. R., & Ma, X. (2007). Influence of citric acid on the properties of glycerol–plasticized dry starch (DTPS) and DTPS/poly(lactic acid) blends. *Starch-Stärke*, 59(9), 409–417. <http://dx.doi.org/10.1002/star.200700617>
- Wang, N., Yu, J., Chang, P. R., & Ma, X. (2008). Influence of formamide and water on the properties of thermoplastic starch/poly(lactic acid) blends. *Carbohydrate Polymers*, 71(1), 109–118. <http://dx.doi.org/10.1016/j.carbpol.2007.05.025>
- Wang, S., Yu, J., & Yu, J. (2004). Influence of maleic anhydride on the compatibility of thermal plasticized starch and linear low-density polyethylene. *Journal of Applied Polymer Science*, 93(2), 686–695. <http://dx.doi.org/10.1002/app.20416>
- Yu, F., Nakamura, N., & Inoue, Y. (2010). Effect of comonomer-unit composition and its distribution of bacterial poly (3-hydroxybutyrate-co-3-hydroxyhexanoate) on miscibility and physical properties of its blend with poly (ethylene oxide). *Polymer*, 51(23), 5556–5566.
- Zeng, J.-B., Jiao, L., Li, Y.-D., Srinivasan, M., Li, T., & Wang, Y.-Z. (2011). Bio-based blends of starch and poly(butylene succinate) with improved miscibility, mechanical properties, and reduced water absorption. *Carbohydrate Polymers*, 83(2), 762–768. <http://dx.doi.org/10.1016/j.carbpol.2010.08.051>